Nanoscale

Cite this: *Nanoscale*, 2011, **3**, 1874

www.rsc.org/nanoscale

PAPER

Covalent immobilization of nisin on multi-walled carbon nanotubes: superior antimicrobial and anti-biofilm properties

Xiaobao Qi, Gunawan Poernomo, Kean Wang, Yuan Chen, Mary B. Chan-Park, Rong Xu and Matthew Wook Chang*

Received 10th January 2011, Accepted 28th January 2011
DOI: 10.1039/c1nr10024f

Despite unique and useful properties of multi-walled carbon nanotubes (MWNTs) such as high strength and a low synthesis cost, their weak antimicrobial property hampers their use as an antimicrobial material. Herein, we demonstrate that the immobilization of nisin, a natural and inexpensive antimicrobial peptide, with poly(ethylene glycol) (PEG_{1000}) as a linker significantly enhanced the antimicrobial and anti-biofilm properties of MWNTs. The MWNT–nisin composite showed up to 7-fold higher antimicrobial property than pristine MWNTs against *Escherichia coli*, *Pseudomonas aeruginosa*, *Staphylococcus aureus* and *Bacillus subtilis*. Moreover, the MWNT–nisin composite had a dramatically improved capability to prevent biofilm formation both on a deposited film and in suspension. In particular, the MWNT–nisin deposit film exhibited a 100-fold higher anti-biofilm property than the MWNT deposit film. Further, it has been shown that PEG and nisin are covalently attached to MWNTs with excellent stability against leaching. We envision that our novel MWNT–nisin composite can serve as an effective and economical antimicrobial material.

Introduction

Infectious diseases are frequently spread through contact with biofilm-contaminated surfaces. The sessile communities of biofilm, which provide protection against antimicrobial agents, are difficult to treat and eventually become persistent transmission sources of infectious diseases.[1] Among the most effective ways to prevent biofilm formation is to interfere with the adhesion of bacteria on the surface,[2] which is a crucial step of colonization.[3,4] Antimicrobial materials equipped with an additional anti-adhesion property will certainly render them wider applications in aerospace systems,[5] defense and biomedical devices,[6] food processing equipment, and food and pharmaceutical packaging.[7]

Carbon nanotubes (CNTs) have been widely used in many composite materials[8,9] because of their unique mechanical and electronic properties.[10] Another useful property of CNTs that has recently been reported is the antimicrobial activity, which causes physical damage to bacterial cells.[11–13] However, this antimicrobial property is frequently compromised because CNTs also strongly adsorb bacterial cells, leading to biofilm formation.[14] Further, multi-walled carbon nanotubes (MWNTs), of which the synthesis cost is much lower than that of single-walled carbon nanotubes (SWNTs), show a very weak antimicrobial property. Among the previous efforts to overcome this problem is to incorporate antimicrobial molecules onto the surface of MWNTs. Despite improved antimicrobial property achieved by immobilizing silver nanoparticles on MWNTs and other materials,[15,16] silver ions are released over time, leading to a gradual loss in the efficiency of the antimicrobial property as well as causing environmental contamination. Antimicrobial peptides (AMPs) are another class of antimicrobial molecules that can potentially be exploited to improve the antimicrobial and anti-adhesion properties of MWNTs. In particular, nisin, a natural and inexpensive AMP, represents a good candidate because it possesses a strong efficacy against a broad range of Gram-positive bacteria, high stability, low toxicity to human, and a low propensity of causing antibiotic resistance. It also exerts strong antimicrobial activity in a nanomolar range and a rapid onset capability of killing bacteria.[17] More importantly, nisin has been utilized as a food preservative for decades, as approved by the United States Food and Drug Administration (FDA).[18] Nisin interferes with cell wall synthesis by binding to the lipid II, a core precursor of cell wall synthesis, and efficiently permeabilizing cell membrane *via* the formation of pores.[19] To achieve an effective bactericidal activity on the MWNT surface, nisin needs to be immobilized with a long flexible linker molecule, providing enough mobile space to pass cell wall and enabling the lateral diffusion of nisin in the lipid bi-layer of cell membrane.[20]

Consequently, in this study, we developed a stable MWNT–nisin composite by covalently immobilizing nisin with poly(ethylene glycol) (PEG) as a linker. Another reason of using PEG

Division of Chemical and Biomolecular Engineering, School of Chemical and Biomedical Engineering, Nanyang Technological University, 62 Nanyang Drive, 637459, Singapore. E-mail: Matthewchang@ntu.edu.sg; Fax: +65 6794 7553; Tel: +65 6513 8063

as a linker was that PEGs reportedly have non-adhesive, non-toxic and non-immunogenic properties.[21] Our novel MWNT–nisin has shown greatly improved antimicrobial and anti-biofilm activity compared to pristine MWNTs.

Materials and methods

MWNTs and strains

Multi-walled carbon nanotubes (MWNTs) (Chengdu Research Institute of Organic Chemistry, China) and nisin ($C_{143}H_{228}O_{37}N_{42}S_7$, Zhejiang Silver Elephant I/E Co. Ltd, China) with a purity of 95% or higher were used for immobilization. Our target bacterial strains, *Escherichia coli* (ATCC 8739), *Pseudomonas aeruginosa* (ATCC 9027), *Staphylococcus aureus* (ATCC 6538) and *Bacillus subtilis* (ATCC 6051), were all obtained from the American Type Culture Collection (ATCC).

Functionalization of MWNTs with carboxyl acid (–COOH) groups

MWNTs were first modified with carboxyl acid groups by using concentrated H_2SO_4 and HNO_3. In brief, MWNTs were calcined in air at 350 °C for 2 hours followed by addition of 50 mL mixture of 98% H_2SO_4 (Normapur) and 69% HNO_3 (Honeywell) (3 : 1, v/v) per 10 mg MWNT.[9] The MWNTs/acids mixture was sonicated at the room temperature for 30 minutes[22] and then refluxed at 110 °C overnight. The MWNTs/acids mixture was then diluted with deionized water, centrifuged, and filtered onto polytetrafluoroethylene (PTFE) membrane (0.2 μm). The resulting slurry was rinsed with deionized water until the pH value of the filtrate reached 7.0. The wet sample was freeze dried for further modification.

Attachment of PEG linker by esterification

The modified MWNTs were grafted with PEG_{1000} (Fluka, $M_w \approx 1000$) as a spacer *via* esterification reaction. Then, 10 mg of the modified MWNTs was added into 50 mL of degassed thionyl chloride (Merck, 99%) and the mixture was refluxed at 70 °C for 6 hours. The excess thionyl chloride was completely eliminated using vacuum evaporation at 70 °C. Through this reaction, the carboxylic groups on the previously modified MWNTs were converted into acid chloride.[23] Subsequently, 10 g of PEG_{1000} was added into a flask containing MWNTs with acid chloride after being dehydrated by rotary evaporation in 100 mL toluene as a solvent. The esterification reaction was carried out in a sealed flask at the room temperature with agitation for 18 hours. The samples were then washed with chloroform several times to remove free PEG_{1000} by centrifugation, followed by washing with deionized water. The resulting MWNTs modified with PEG linker were freeze dried for further modification.

Nisin attachment to MWNT–PEG

MWNT–PEG was linked with nisin using hexamethylene diisocyanate (Fluka, 99%) as a coupling agent and dibutyltin dilaurate (Aldrich, 95%) as a catalyst. Then, 10 mg of MWNT–PEG was dispersed in 20 mL of dimethylformamide (DMF, Normapur, 99.8%) by sonication. The resulting suspension was slowly added into 30 mL of DMF containing 1 mL of hexamethylene diisocyanate and 50 μL of dibutyltin dilaurate with stirring in a sealed flask.[24] The reaction was conducted in an ice bath for 4 hours and at the room temperature for 1 hour. The obtained samples were washed with DMF and centrifuged four times to remove the residual reagents. Further, 0.5 g of dehydrated nisin was quickly added into 30 mL DMF containing the MWNTs described above and the nisin grafting reaction was conducted in a shaking incubator at 37 °C for overnight. After centrifugation, the samples were filtrated and washed thoroughly with deionized water to remove any unreacted nisin until the UV absorbance peak at 214 nm was not observed.

Characterization

Thermogravimetric analysis (TGA) was conducted with PerkinElmer Diamond TGA/DTA (MA, USA) with a heating rate of 20 °C min^{-1} from 50 to 500 °C in nitrogen atmosphere. Field-emission scanning electron microscopy (FESEM) was carried out with JEOL FESEM JSM-6700 (Tokyo, Japan). Fourier transform infrared (FTIR) spectra were obtained using PerkinElmer Paragon 1000 Spectra (MA, USA).

MWNT–nisin antimicrobial activity against planktonic bacteria

Antimicrobial testing was conducted as described by Yuan *et al.*[15] The target bacteria were cultured to a mid-log phase at 37 °C with shaking. The cells were harvested by centrifugation, washed, and suspended in phosphate buffer saline (PBS) to approximately 10^7 colony forming units (CFUs) per mL. MWNT–nisin samples were diluted in PBS to a desired concentration for antimicrobial testing. Then, 20 μL of the cell suspension in PBS and 1 mL of the MWNT–nisin suspension were mixed and incubated at 37 °C for 1 hour. The samples were then transferred to neutralization broth and plated on tryptic soy agar at 37 °C by ten-fold dilution. The numbers of the viable cells were determined by colony counting and 1 mL of pure PBS was used as a negative control. Bacterial killing percentage (%kill) was defined as $(N_{PBS} - N_{sample})/N_{PBS} \times 100$, where N_{PBS} and N_{sample} represent the number of bacteria in PBS and the sample, respectively.

MWNT–nisin antimicrobial activity against biofilm formation

S. aureus was cultured to a mid-log phase in Mueller–Hinton broth (MHB) and washed twice and resuspended in MHB. After incubation with MWNT–nisin at 37 °C for 18 hours, the cells were washed three times to remove free-suspended cells. The biofilm was stained with crystal violet for 1 hour and was rinsed with water five times to remove crystal violet residue. Crystal violet dyes were extracted with an ethanol and acetone mixture (8 : 2, v/v), and the absorbance was measured at 595 nm using a microplate reader (Bio Tek Instruments).[25] All experiments were conducted with eight biological replicates with four technical replicates each, and the statistical significance was determined by using the Student's *t* test.

MWNT–nisin anti-adhesion activity

MWNT–nisin was dispersed in DMF and filtered onto PTFE membrane with a density of 0.3 mg cm^{-2}, which allows a full

coverage and good permeability.[26] The samples were washed with 250 mL ethanol to remove DMF and ethanol was subsequently removed with 400 mL deionized water by filtration. *P. aeruginosa* and *S. aureus* were cultured to a mid-log phase in MHB, washed twice, and resuspended in fresh MHB to an optical density of 0.05 at 600 nm, which is corresponding to about 3×10^7 CFU mL^{-1}. Then, 4 mL of the cell suspension with fresh broth was spread onto the surface of the deposited film of MWNT–nisin. After incubation for 3 hours at 37 °C, the samples were gently rinsed three times with sterile PBS to remove non-adherent bacteria.[27] Finally, the sessile viable cells on the MWNT–nisin deposit film were enumerated by the decimal dilution plating method after 5 minutes of sonication. The percentage of anti-adhesion was defined as $(N_{MWNTs} - N_{MWNT-nisin})/N_{MWNTs} \times 100$, where N_{MWNTs} and $N_{MWNT-nisin}$ are the viable cell numbers from MWNTs and MWNT–nisin, respectively. Each experiment was repeated three times. A confocal laser scanning microscope (CLSM) (LSM510; Zeiss, Thornwood, NY) was used to obtain a direct image of the attached cells after SYTO 9 (Invitrogen, Carlsbad, CA) staining. *Z*-Stack was developed by scanning per μm. For image capture, the excitation and emission wavelengths were set at 488 and 530 nm, respectively. Two-dimensional (2D) images were obtained using LSM Image Brower software. Both MWNTs and MWNT–PEG were used as negative controls.

Nisin detection

Untreated and leached nisin was analyzed by using high performance liquid chromatography (HPLC) (Agilent 1100 series, CA, USA) with a Phenomenex (4.6 by 250 cm column; 4 μm particle size) C_{18} reverse-phase column. Linear gradients of 0.1% aqueous trifluoroacetic acid and 0.1% trifluoroacetic acid in CH_3CN were run from 0.98 : 0.02 to 0 : 1 over 100 min with UV detection at 214 nm and 5 μL input volume per sample.[28]

Morphological change observation by scanning electron microscopy

Field Emission Scanning Electron Microscopy (FESEM) was used to observe the change in cellular morphology upon exposure to MWNT–nisin deposited film. *P. aeruginosa* and *S. aureus* were incubated on the deposited films of MWNTs and MWNT–nisin for 1 hour, and then fixed with 4% gluteraldehyde in 0.15 M sodium phosphate buffer (pH 7.4). The fixed-cell films were dehydrated using ethanol with ascending concentrations (30–100%) three times at respective concentrations. Subsequently, the slides with the film were dried at 60 °C for 4 hours, coated with a platinum metal for 60 seconds at 20 mA, and transferred to FESEM for imaging.

Results

Fig. 1 summarizes the synthesis steps of the MWNT–nisin composite as described in Materials and methods. To verify the attachment of nisin on MWNTs after the synthesis, the absorption peaks of nisin functional groups immobilized on MWNTs were identified using FTIR spectra. As shown in Fig. 2, the FTIR spectra indicate that MWNT–nisin exhibited strong characteristic peaks of amide groups at 1654 and 1530 cm^{-1}, which are attributed to amide I (C═O stretching vibration) and amide II (N–H bending and C–N stretching) groups of nisin.[29] The presence of PEG as a linker was indicated by a broad band at around 1065 cm^{-1} which is attributed to the C–C–O– stretching vibration. The same band was also observed for MWNT–nisin, but was absent in the spectrum of MWNT–COOH. The latter mainly exhibited the COOH stretching vibration at around 1729 cm^{-1}. Furthermore, to confirm that the attachment of PEG and nisin was due to surface layer modification, samples of MWNTs, MWNT–PEG and MWNT–nisin were examined using FESEM. Fig. 3 shows no apparent polymer layers on the surface of MWNT–PEG and MWNT–nisin. In addition, no morphology change between MWNTs, MWNT–PEG, and MWNT–nisin was observed. Hence, these results suggest that our synthesis procedures successfully led to the covalent immobilization of nisin onto MWNTs with PEG_{1000} as a linker.

To determine the percentage of immobilized nisin on the composite, TGA analysis was performed. Fig. 4 displays the weight loss profiles of MWNT–COOH, MWNT–PEG, and MWNT–nisin during a temperature increase from the room temperature to 600 °C. These results suggest that the decomposition onset temperature (T_{onset}) of PEG and nisin was approximately 230 °C. The organic content in each sample was estimated based on the residual weight at 600 °C after the subtraction of the weight percentage of the adsorbed water (up to 200 °C). The estimated weight percentages of organic contents in MWNT–COOH, MWNT–PEG, and MWNT–nisin were 10.15%, 23.80%, and 46.94%, respectively. Therefore, the estimated total percentage of nisin, hexamethylene diisocyanate and PEG in MWNT–nisin was about 36.79% (*i.e.* 46.94% − 10.15%).

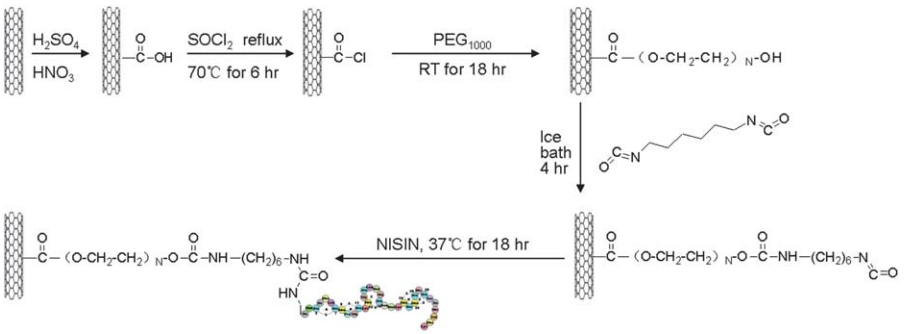

Fig. 1 Schematic illustration of surface modification of MWNTs to generate MWNT–nisin composite with PEG_{1000} as a linker.

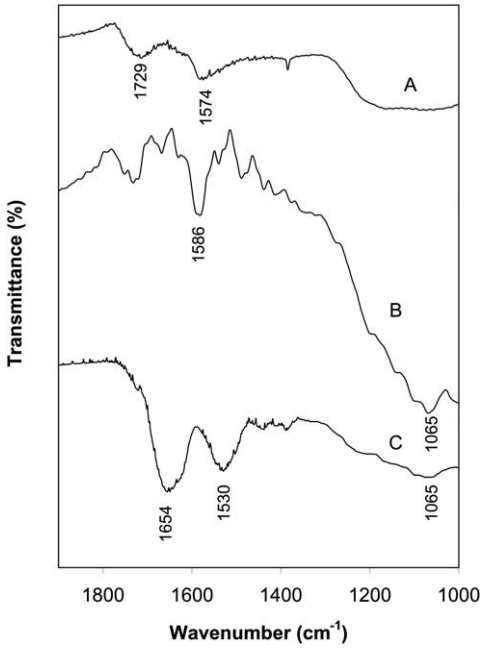

Fig. 2 FTIR spectra of MWNT–COOH (A), MWNT–PEG (B) and MWNT–nisin (C).

Assuming that all PEG molecules were attached with nisin through the diisocyanate group, the percentage of nisin in MWNT–nisin can be estimated to be 27.29% using the following equation:

(Molecular weight of nisin/molecular weights of nisin, diisocyanate and PEG) × 36.79%

where the molecular weights of nisin, diisocyanate and PEG are 3354, 168 and 1000 respectively.

Alternatively, as the total percentage of nisin and hexamethylene diisocyanate was calculated to be 23.14% (46.94% – 23.80%), the percentage of nisin can be estimated to be 22.04% again by assuming that all hexamethylene diisocyanate molecules were reacted with nisin. As such, the discrepancy found based on the two calculations could be mainly due to the above mentioned assumptions. In the actual process, incomplete reactions between PEG and hexamethylene diisocyanate, and between hexamethylene diisocyanate and nisin likely occurred. Furthermore, the percentage of carbon atoms of MWNTs grafted with the carboxylic group can be estimated to be 3.01% (*i.e.* (10.15%/45 (molecular weight of COOH))/((1–10.15%)/12

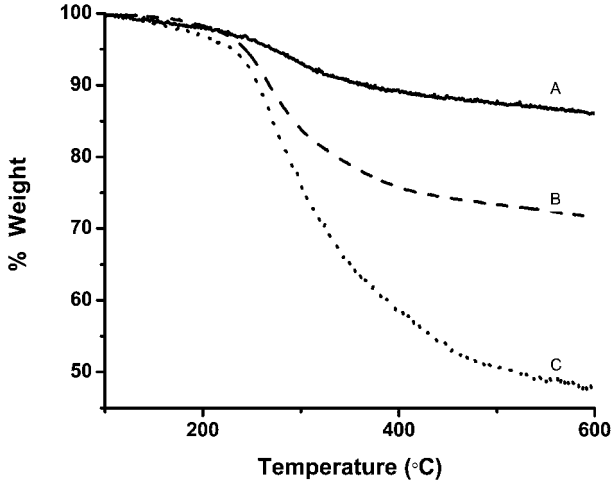

Fig. 4 TGA curves of MWNT–COOH (A), MWNT–PEG (B), and MWNT–nisin (C).

(molecular weight of C))). However, the percentage of carbon atoms eventually attached with PEG *via* the esterification reaction was only 0.36% (*i.e.* (23.8%/(1000 – 18 + 45) (graft PEG molar quantity))/((1–23.8%)/12)). These results imply that the immobilization efficiency of nisin is controlled by the efficiency of the esterification reaction for PEG linker attachment.

To evaluate how the covalent immobilization of nisin affected the antimicrobial activity of MWNTs, we then compared the bactericidal activity of nisin, MWNTs, and MWNT–nisin against two Gram-negative bacteria (*E. coli* and *P. aeruginosa*) and two Gram-positive bacteria (*S. aureus* and *B. subtilis*). Each of the bacteria was exposed to MWNTs and MWNT–nisin at 10 and 100 μg mL^{-1}. Further, based on the earlier estimation that MWNT–nisin contained 27.29% of nisin (a higher value was used in order to assure that the performance of MWNT–nisin was not overestimated against that of free nisin), we also evaluated the bactericidal activity of 2.73 and 27.29 μg mL^{-1} of free nisin for comparison. Fig. 5 shows that nisin immobilization significantly increased the bactericidal activity of MWNTs 1.5- to 7-fold. While this increase was more evident against the Gram-positive strains (*i.e. S. aureus* and *B. subtilis*), 100 μg mL^{-1} of MWNT–nisin showed at least 80% kill against the test strains. Even at 10 μg mL^{-1}, MWNT–nisin exhibited higher than 90% kill against *S. aureus* and *B. subtilis*. These results also suggest that although the antimicrobial activity of MWNT–nisin was weaker than that of nisin at the corresponding concentrations (*i.e.* 100 *vs.* 27.29 and 10 *vs.* 2.73 μg mL^{-1}) as expected, at least 90% of the

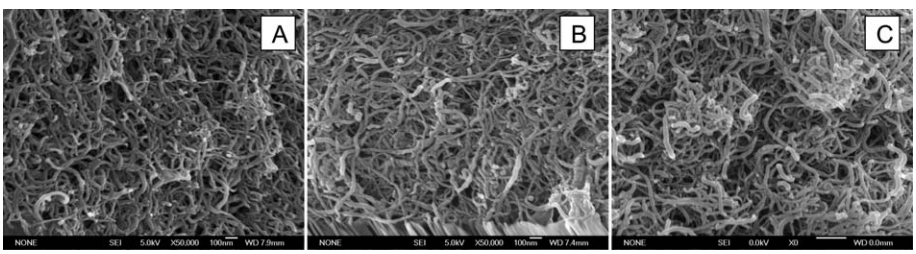

Fig. 3 FESEM images of MWNTs (A), MWNT–PEG (B) and MWNT–nisin (C).

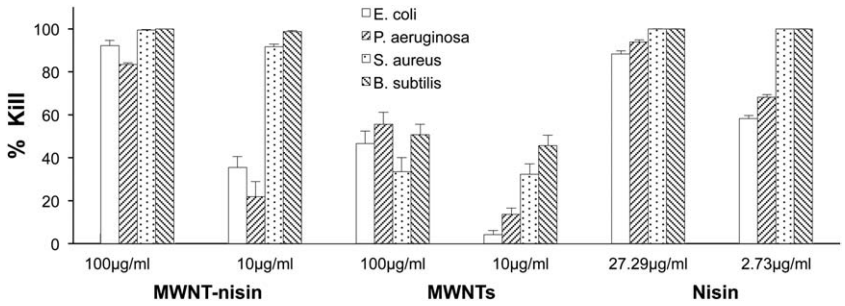

Fig. 5 Killing percentages of MWNTs (10 and 100 μg mL^{-1}), MWNT–nisin (10 and 100 μg mL^{-1}) and nisin (2.73 and 27.29 μg mL^{-1}), where PBS was used as the negative control.

bactericidal activity of nisin was indeed retained at 100 μg mL^{-1} MWNT–PEG–nisin.

Then, to evaluate the antimicrobial activities of MWNT–nisin on a deposited film, MWNT–nisin was deposited onto a membrane, and after 1 hour incubation with bacteria suspension, live cells on the membrane were examined using confocal laser microscopy. Fig. 6 shows that *P. aeruginosa* and *S. aureus* on the MWNT–nisin deposit were mostly stained red (PI staining indicates dead cells), whereas the cells on MWNTs and MWNT–PEG were stained green (SYTO 9 staining indicates live cells). This result suggests that MWNT–nisin possessed a strong bactericidal activity in a deposited form.

Then, to assess the ability of MWNT–nisin to inhibit biofilm formation, we exposed *S. aureus* to a range of concentrations of MWNT–nisin in suspension (1.25, 2.5, 5 and 10 μg mL^{-1}). Note that the minimum inhibitory concentration (MIC) of MWNT–nisin was 10 μg mL^{-1}; thus, 10 μg mL^{-1} led to no visible planktonic cell growth after overnight incubation, whereas the cell growth was evident at 2.5 and 5 μg $mL.^{-1}$ Fig. 7 shows that nisin immobilization significantly improved the inhibitory effect of MWNTs on biofilm formation. While MWNT suspension alone also decreased biofilm formation by approximately 37%, nisin immobilization resulted in 95% reduction in biofilm formation in suspension. Another notable observation was that a strong anti-biofilm activity was achieved even at below MIC (*i.e.* at 1.25, 2.5 and 5 μg mL^{-1}). This outcome implies that biofilm formation was strongly retarded without the growth inhibition of *S. aureus*, potentially contributed to by the anti-adhesion property of MWNT–nisin.

Therefore, to determine how nisin immobilization improved the anti-adhesion property of MWNTs, we enumerated the viable cells adhering to the deposited film of MWNTs, MWNT–PEG, and MWNT–nisin after a 3 hour incubation at 37 °C. Table 1 shows that the MWNT–nisin deposit film had approximately 100 times fewer cells on the surface than the MWNTs and MWNT–PEG deposit film. Further, to examine the cells adhering to the MWNTs and MWNT–nisin deposit films, we visualized the live cells of *P. aeruginosa* and *S. aureus* on the surface using confocal laser microscopy. Fig. 8 shows that *P. aeruginosa* and *S. aureus* created a thick and complex biofilm structure on the MWNT deposit film, whereas few live cells remained on the MWNT–nisin deposit film. Our results here clearly indicate that nisin immobilization dramatically improved the anti-adhesion property of MWNTs.

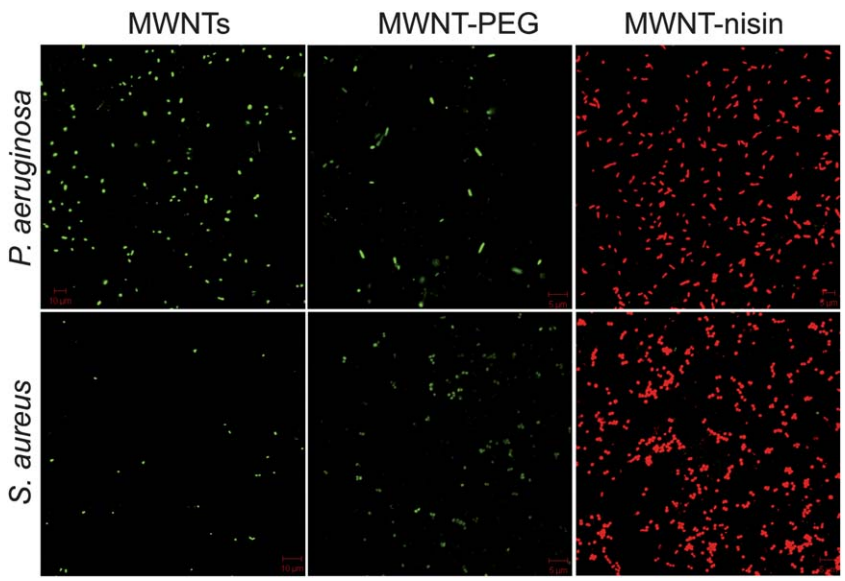

Fig. 6 Representative confocal scanning laser microscopy images of attached *P. aeruginosa* and *S. aureus* on MWNTs, MWNT–PEG, and MWNT–nisin after 1 hour incubation.

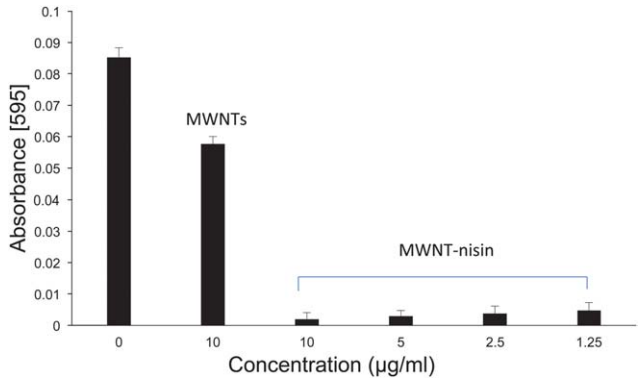

Fig. 7 Analysis of biofilm formation in the presence of MWNTs and MWNT–nisin (**, $p < 0.01$, compared to MWNTs).

Table 1 The anti-adhesion property of MWNT–nisin deposit film compared to MWNTs and MWNT–PEG deposit films

Material	%Anti-adhesion[a]
MWNT–nisin (*vs.* MWNTs)	99.92 ± 0.13
MWNT–nisin (*vs.* MWNT–PEG)	99.1 ± 0.15

[a] %Anti-adhesion = (N_{MWNTs} or $N_{MWNT-PEG}$ − $N_{MWNT-nisin}$)/(N_{MWNTs} or $N_{MWNT-PEG}$) × 100, where N_{MWNTs}, $N_{MWNT-PEG}$, and $N_{MWNT-nisin}$ are the viable cell numbers from MWNTs, MWNT–PEG, and MWNT–nisin samples.

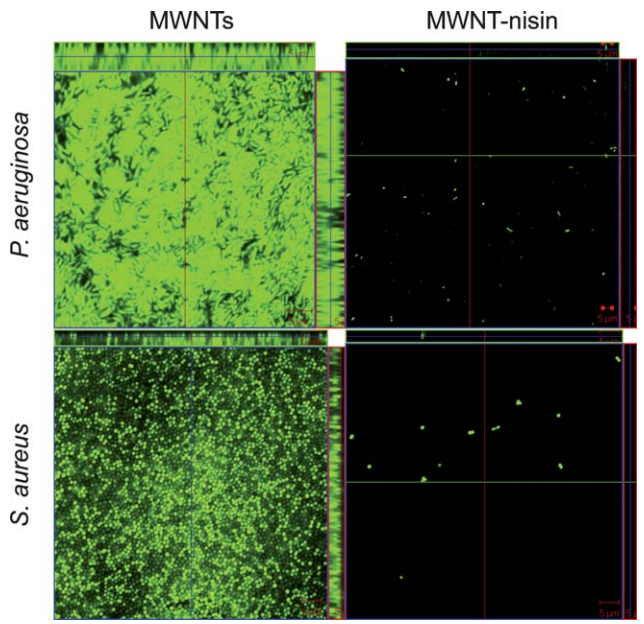

Fig. 8 Representative confocal scanning laser microscopy images of *P. aeruginosa* and *S. aureus* on the MWNTs and MWNT–nisin after a 3 hour incubation.

Lastly, to confirm that the antimicrobial activity described above resulted from immobilized nisin, and to evaluate the stability of nisin immobilization on MWNTs, nisin leaching from MWNT–nisin was quantified using chromatographic HPLC. Fig. 9 shows that no apparent leaching of nisin was observed from MWNT–nisin after 1 hour incubation with *S. aureus*.

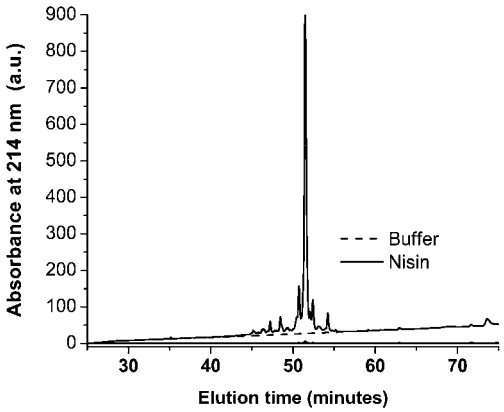

Fig. 9 The reverse phase (RP)-HPLC results of nisin and buffer solutions. Buffer represents the treatment solution after 1 hour incubation with *S. aureus* (10^5 CFU mL^{-1}) at 37 °C. Nisin solution (20 μg mL^{-1}) was used as a positive control.

This result indicates that the antimicrobial activity of MWNT–nisin was due to the immobilized nisin, not leached nisin. In addition, we also confirmed that the antimicrobial activity of the MWNT–nisin suspension was retained for over 60 days at the room temperature (data not shown), implying that MWNT–nisin is a stable antimicrobial material due to covalently immobilized nisin on MWNTs.

Discussion

MWNTs possess a limited antimicrobial property, inadequate for preventing biofilm formation on the surface. In this study, we significantly improved the antimicrobial and anti-adhesion properties of MWNTs by immobilizing nisin with PEG as a linker. Our novel MWNT–nisin composite showed 1.5 to 7 times higher bactericidal activity against *E. coli*, *P. aeruginosa*, *B. subtilis*, and *S. aureus* planktonic cells than MWNTs. Further, the anti-biofilm activity was enhanced 100-fold on the MWNT–nisin deposit film and 2.6-fold in MWNT–nisin suspension. Even compared to pure nisin, MWNT–nisin at 100 μg mL^{-1} retained at least 90% of the antimicrobial activity of nisin against all four target pathogens.

The most impressive characteristic of our MWNT–nisin is its strong anti-adhesion and anti-biofilm activity. Even at the lower-than-MIC concentrations (*i.e.* 1.25, 2.5, and 5 μg mL^{-1}), which caused no visual growth of *S. aureus*, MWNT–nisin effectively prevented biofilm formation in suspension. Moreover, the MWNT–nisin deposit film showed 100-times higher anti-biofilm property than the MWNT deposit film. The formation of bacterial biofilm reportedly takes place over at least three stages: initial adsorption, irreversible adhesion to the surface, and colonization.[30] Considering these three stages, the strong anti-biofilm activity of our MWNT–nisin may be contributed to by the following: (i) the initial attachment of bacterial cells to MWNT–nisin might significantly be reduced because of the strong antimicrobial effect and/or (ii) bacterial twitching motility, required for biofilm formation on the surface, might be limited because MWNT–nisin interacts with bacterial cells.[31,32]

In conclusion, herein, we developed an efficient and economical method to prepare MWNTs with superior antimicrobial

property. This newly developed MWNT–nisin with PEG linker displays far stronger antibacterial and anti-adhesion activities. Moreover, nisin molecules are stably immobilized onto MWNTs without undergoing leaching for at least sixty days. Moreover, most of the chemicals used in the synthesis are nontoxic, biocompatible, and relatively inexpensive compared to other similar synthesis methods. In addition, the immobilization process is simple and thus, can be expanded to MWNT–nisin production at a larger scale. We envision that our MWNT–nisin will serve as an effective and economical antimicrobial material.

Acknowledgements

This research was funded by Environment and Water Industry Programme Office (EWI)—National Research Foundation, Singapore, through Project no.: 0802-IRIS-12.

Reference

1 S. Hota, Z. Hirji, K. Stockton, C. Lemieux, H. Dedier and G. Wolfaardt, et al., Outbreak of multidrug-resistant *Pseudomonas aeruginosa* colonization and infection secondary to imperfect intensive care unit room design, *Infect. Contr. Hosp. Epidemiol.*, 2009, **30**(1), 25–33.

2 J. Kim, B. Pitts, P. S. Stewart, A. Camper and J. Yoon, Comparison of the antimicrobial effects of chlorine, silver ion, and tobramycin on biofilm, *Antimicrob. Agents Chemother.*, 2008, **52**(4), 1446–1453.

3 M. R. Parsek and T. Tolker-Nielsen, Pattern formation in *Pseudomonas aeruginosa* biofilms, *Curr. Opin. Microbiol.*, 2008, **11**(6), 560–566.

4 Z. Qin, X. Yang, L. Yang, J. Jiang, Y. Ou and S. Molin, et al., Formation and properties of *in vitro* biofilms of ica-negative *Staphylococcus epidermidis* clinical isolates, *J. Med. Microbiol.*, 2007, **56**(Pt 1), 83–93.

5 J. W. Wilson, C. M. Ott, K. Honer zu Bentrup, R. Ramamurthy, L. Quick and S. Porwollik, et al., Space flight alters bacterial gene expression and virulence and reveals a role for global regulator Hfq, *Proc. Natl. Acad. Sci. U. S. A.*, 2007, **104**(41), 16299–16304.

6 R. O. Darouiche, M. D. Mansouri and M. J. Schneidkraut, Comparative efficacies of telavancin and vancomycin in preventing device-associated colonization and infection by *Staphylococcus aureus* in rabbits, *Antimicrob. Agents Chemother.*, 2009, **53**(6), 2626–2628.

7 D. S. Cha and M. S. Chinnan, Biopolymer-based antimicrobial packaging: a review, *Crit. Rev. Food Sci. Nutr.*, 2004, **44**(4), 223–237.

8 W. Ma, L. Liu, Z. Zhang, R. Yang, G. Liu and T. Zhang, et al., High-Strength composite fibers: realizing true potential of carbon nanotubes in polymer matrix through continuous reticulate architecture and molecular level couplings, *Nano Lett.*, 2009, **9**(8), 2855–2861.

9 J. F. Che, W. Yuan, G. H. Jiang, J. Dai, S. Y. Lim and M. B. Chan-Park, Epoxy composite fibers reinforced with aligned single-walled carbon nanotubes functionalized with generation 0-2 dendritic poly(amidoamine), *Chem. Mater.*, 2009, **21**(8), 1471–1479.

10 M. Terada, S. Abe, T. Akasaka, M. Uo, Y. Kitagawa and F. Watari, Multiwalled carbon nanotube coating on titanium, *Bio-med. Mater. Eng.*, 2009, **19**(1), 45–52.

11 S. Kang, M. Pinault, L. D. Pfefferle and M. Elimelech, Single-walled carbon nanotubes exhibit strong antimicrobial activity, *Langmuir*, 2007, **23**(17), 8670–8673.

12 S. Kang, M. Herzberg, D. F. Rodrigues and M. Elimelech, Antibacterial effects of carbon nanotubes: size does matter!, *Langmuir*, 2008, **24**(13), 6409–6413.

13 S. Kang, M. S. Mauter and M. Elimelech, Physicochemical determinants of multiwalled carbon nanotube bacterial cytotoxicity, *Environ. Sci. Technol.*, 2008, **42**(19), 7528–7534.

14 T. Akasaka and F. Watari, Capture of bacteria by flexible carbon nanotubes, *Acta Biomater.*, 2009, **5**(2), 607–612.

15 W. Yuan, G. H. Jiang, J. F. Che, X. B. Qi, R. Xu and M. W. Chang, et al., Deposition of silver nanoparticles on multiwalled carbon nanotubes grafted with hyperbranched poly(amidoamine) and their antimicrobial effects, *J. Phys. Chem. C*, 2008, **112**(48), 18754–18759.

16 D. Roe, B. Karandikar, N. Bonn-Savage, B. Gibbins and J. B. Roullet, Antimicrobial surface functionalization of plastic catheters by silver nanoparticles, *J. Antimicrob. Chemother.*, 2008, **61**(4), 869–876.

17 S. M. Asaduzzaman, J. Nagao, H. Iida, T. Zendo, J. Nakayama and K. Sonomoto, Nukacin ISK-1, a bacteriostatic lantibiotic, *Antimicrob. Agents Chemother.*, 2009, **53**(8), 3595–3598.

18 E. Breukink, I. Wiedemann, C. van Kraaij, O. P. Kuipers, H. G. Sahl and B. de Kruijff, Use of the cell wall precursor lipid II by a pore-forming peptide antibiotic, *Science*, 1999, **286**(5448), 2361–2364.

19 A. Peschel and H. G. Sahl, The co-evolution of host cationic antimicrobial peptides and microbial resistance, *Nat. Rev. Microbiol.*, 2006, **4**(7), 529–536.

20 M. Bagheri, M. Beyermann and M. Dathe, Immobilization reduces the activity of surface-bound cationic antimicrobial peptides with no influence upon the activity spectrum, *Antimicrob. Agents Chemother.*, 2009, **53**(3), 1132–1141.

21 W. S. Bae and M. W. Urban, Creating patterned poly(dimethylsiloxane) surfaces with amoxicillin and poly(ethylene glycol), *Langmuir*, 2006, **22**(24), 10277–10283.

22 M. W. Marshall, S. Popa-Nita and J. G. Shapter, Measurement of functionalised carbon nanotube carboxylic acid groups using a simple chemical process, *Carbon*, 2006, **44**(7), 1137–1141.

23 N. Aumsuwan, S. Heinhorst and M. W. Urban, The effectiveness of antibiotic activity of penicillin attached to expanded poly(tetrafluoroethylene) (ePTFE) surfaces: a quantitative assessment, *Biomacromolecules*, 2007, **8**(11), 3525–3530.

24 J. Yuan, L. Chen, X. Jiang, J. Shen and S. Lin, Chemical graft polymerization of sulfobetaine monomer on polyurethane surface for reduction in platelet adhesion, *Colloids Surf., B*, 2004, **39**(1–2), 87–94.

25 J. Overhage, A. Campisano, M. Bains, E. C. Torfs, B. H. Rehm and R. E. Hancock, Human host defense peptide LL-37 prevents bacterial biofilm formation, *Infect. Immun.*, 2008, **76**(9), 4176–4182.

26 A. S. Brady-Estevez, S. Kang and M. Elimelech, A single-walled-carbon-nanotube filter for removal of viral and bacterial pathogens, *Small*, 2008, **4**(4), 481–484.

27 K. Glinel, A. M. Jonas, T. Jouenne, J. Leprince, L. Galas and W. T. S. Huck, Antibacterial and antifouling polymer brushes incorporating antimicrobial peptide, *Bioconjugate Chem.*, 2009, **20**(1), 71–77.

28 E. Chollet, I. Sebti, A. Martial-Gros and P. Degraeve, Nisin preliminary study as a potential preservative for sliced ripened cheese: NaCl, fat and enzymes influence on nisin concentration and its antimicrobial activity, *Food Control*, 2008, **19**(10), 982–989.

29 G. Socrates, *Infrared Characteristic Group Frequencies*, John Wiley & Sons, 2nd edn, 2004.

30 R. Kolter and E. P. Greenberg, Microbial sciences—The superficial life of microbes, *Nature*, 2006, **441**(7091), 300–302.

31 O. Bahar, T. Goffer and S. Burdman, Type IV Pili are required for virulence, twitching motility, and biofilm formation of *Acidovorax avenae subsp. citrulli*, *Mol Plant-Microbe Interact.*, 2009, **22**(8), 909–920.

32 J. J. Varga, B. Therit and S. B. Melville, Type IV pili and the CcpA protein are needed for maximal biofilm formation by the Gram-positive anaerobic pathogen *Clostridium perfringens*, *Infect. Immun.*, 2008, **76**(11), 4944–4951.

